DEPENDENCE OF PROTON PRODUCTION ON CENTRALITY IN AU–AU COLLISIONS AT HIGH ENERGIES

Fu-Hu Liu

Institute of Modern Physics, Shanxi Teachers University
Linfen, Shanxi 041004, China

and

China Center of Advanced Science and Technology (World Laboratory)
Beijing 100080, China
e-mail: liufh@dns.sxtu.edu.cn

(Received July 20, 2004)

The rapidity distributions of protons produced in Au–Au collisions at the Alternating Gradient Synchrotron (AGS) energies are investigated by a two-cylinder model. The different distribution shapes for different centrality cuts are mainly determined by different contributions of leading protons. The cylinders contribute the same distribution shape for different centrality cuts. The calculated results are compared and found to be in agreement with the experimental data of the E917 Collaboration.

PACS numbers: 25.75.–q, 24.10.Pa

In high-energy nucleus–nucleus collisions, a lot of particles are produced in final state [1–3]. This phenomenon is called multiparticle production [4–6]. There are many protons among final state particles [7–9]. These protons are from projectile and target nuclei [10–12]. According to the participant–spectator model [13], some of the final state protons are from participant and others are from spectator.

The rapidity (or pseudorapidity) distributions of final state protons produced in high-energy nucleus–nucleus collisions can be measured in experiment. It is convenient for us to understand the particle production process of interacting system by using the rapidity distributions. A lot of models, for example the microscopic model based on parton substructure [14, 15], multi-phase transport model [16,17], relativistic quantum molecular dynamics model [18, 19], and fireball model [20, 21] *etc.*, have been introduced to describe the rapidity distributions.

In our previous work [22–24], a cylinder model is introduced to describe the rapidity (or pseudorapidity) distributions. Recently, the cylinder model is revised to a two-cylinder model [25–27] and an overlapping cylinder model [28]. The revised cylinder model contains the previous cylinder model, and the temperature of emission source is considered. Because the overlapping cylinder model contains two cylinders, it is in fact a two-cylinder model.

Recently, the Alternating Gradient Synchrotron (AGS) at Brookhaven National Laboratory (BNL) was run at lower energies. The E917 Collaboration reported the rapidity distributions of protons produced in Au–Au collisions at different centralities at 6, 8, and 10.8AGeV [29]. It is obvious that the rapidity distribution shapes are different for different centrality cuts. In this work, we shall use the two-cylinder model to analyze the dependence of proton production on centrality in Au–Au collisions at the lower AGS energies and give an explanation for the rapidity distribution shape of final state protons.

Let us consider the process of high-energy nucleus–nucleus collisions. In the center-of-mass reference frame or in the laboratory reference frame, a projectile nucleus and a target nucleus are expected to make a cylindrical cut through each other along the direction of the incident projectile and form participant. The residual parts of the two nuclei remain relatively undisturbed forming spectators. In rapidity space, the participant projectile (*i.e.* projectile cylinder) lies in the rapidity range $[y_{P\,\mathrm{min}}, y_{P\,\mathrm{max}}]$, and the participant target (*i.e.* target cylinder) lies in the rapidity range $[y_{T\,\mathrm{min}}, y_{T\,\mathrm{max}}]$. The rapidity of the center-of-mass system of collisions is y_{cm} (in the center-of-mass reference frame $y_{\mathrm{cm}} = 0$). The emission points with the same rapidity, y_x, in the cylinder cut region form an emission source in the rapidity space.

In the concerned reference frame, let Δy denote the rapidity shift of the centers of projectile and target cylinders, Dy denote the rapidity shift of the leading projectile and target protons, and $\delta y \equiv (y_{P\,\mathrm{max}} - y_{P\,\mathrm{min}})/2 = (y_{T\,\mathrm{max}} - y_{T\,\mathrm{min}})/2$. In the rest frame of emission source, we assume that the three momentum components p_x^*, p_y^*, and p_z^* obey Gaussian distribution having the same width $\sigma = \sqrt{mT}$, where m and T are the rest mass of proton and the temperature of emission source, respectively. The pseudorapidity η^* is defined by

$$\eta^* \equiv -\ln \tan \frac{\theta^*}{2} = -\ln \tan\left(\frac{1}{2} \arctan \frac{p_{\mathrm{T}}^*}{p_z^*}\right), \tag{1}$$

where θ^* is the emission angle and $p_{\mathrm{T}}^* \equiv \sqrt{p_x^{*2} + p_y^{*2}}$ is the transverse momentum of the concerned particle. The rapidity y^* can be given by [30]

$$y^* = \frac{1}{2}\ln\left(\frac{\sqrt{p_{\mathrm{T}}^{*2}\cosh^2\eta^* + m^2} + p_{\mathrm{T}}^*\sinh\eta^*}{\sqrt{p_{\mathrm{T}}^{*2}\cosh^2\eta^* + m^2} - p_{\mathrm{T}}^*\sinh\eta^*}\right). \tag{2}$$

In the center-of-mass reference frame or in the laboratory reference frame, the rapidity y can be obtained simply by

$$y = y^* + y_x\,. \tag{3}$$

For the projectile and target cylinders, the values of y_x are in the ranges $[\Delta y - \delta y, \Delta y + \delta y]$ and $[-\Delta y - \delta y, -\Delta y + \delta y]$, respectively. For the leading projectile and target protons, the values of y_x are equal to Dy and $-Dy$, respectively. For symmetrical collisions such as Au–Au collisions, the contributions of leading projectile and target protons are equal to each other, and the contributions of the two cylinders are equal to each other, too. Let k denote the contribution of leading projectile or target protons, then the contribution of projectile or target cylinder is $(1-2k)/2$.

A Monte Carlo method is used to calculate the rapidity distribution. The first step, according to the different contributions of leading protons and cylinders, and the distribution range of y_x, the emission source with rapidity y_x is given. The second step, according to the Gaussian p_z^* and Rayleigh p_T^* distributions, the value of η^* is defined. The third step, according to Eqs. (2) and (3), the value of y is obtained. Repeating calculation can give a lot of final state protons with different y. Then the rapidity distribution can be given by a statistical method.

Figure 1 presents the rapidity $(y - y_{\mathrm{cm}})$ distributions, dN/dy, in the center-of-mass reference frame for protons produced in Au–Au collisions at $6A$GeV, where y is the rapidity in the laboratory reference frame. The centrality cuts are shown in the figure. The full circles are the experimental data of the E917 Collaboration [29] and the open circles are reflected around $y = y_{\mathrm{cm}}$ [29]. The experimental data are compared with the Monte Carlo results with 10^6 protons generated for each centrality cut, respectively, using our model code. The curves in Fig. 1 represent the rapidity distributions from the two-cylinder model, which are in good agreement with the E917 experimental data. In the calculation, the parameter values obtained by fitting the experimental data are $T = 150$ MeV, $\Delta y = \delta y = 0.560$, and $Dy = 1.120$. For the centrality cuts from 0–5% to 39–81%, the contributions of leading projectile or target protons are taken as $k = 0.03$, 0.08, 0.12, 0.18, and 0.23 with χ^2/degrees of freedom (dof) of 0.065, 0.026, 0.025, 0.045, and 1.188, respectively.

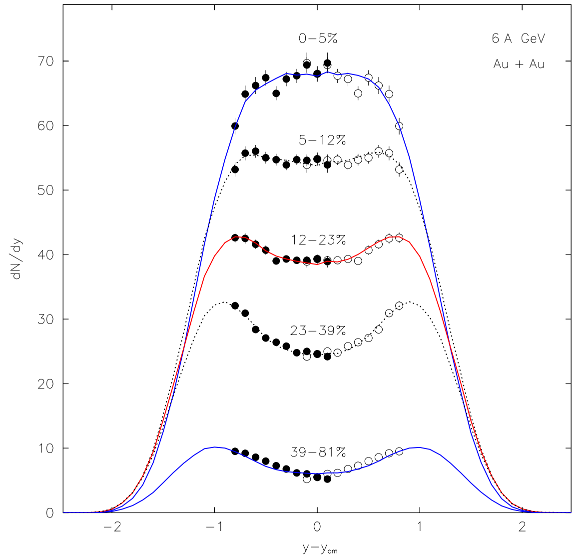

Fig. 1. Rapidity distribution of protons produced in Au–Au collisions at $6A$GeV. The full circles are the experimental data measured by the E917 Collaboration [29] and the open circles are reflected around $y = y_{\rm cm}$ [29]. The curves are our calculated results.

Figure 2 is similar to Fig. 1, but the incident energy is $8A$GeV. The meanings of symbols and curves are the same as those in Fig. 1. In the calculation, the parameter values obtained by fitting the experimental data are $T = 160$ MeV, $\Delta y = \delta y = 0.575$, and $Dy = 1.150$. For the centrality cuts from 0–5% to 39–81%, the contributions of leading projectile or target protons are taken as $k = 0.05$, 0.09, 0.12, 0.17, and 0.24 with χ^2/dof of 0.062, 0.054, 0.032, 0.044, and 0.259, respectively.

Figure 3 is similar to Fig. 1, too, but the incident energy is $10.8A$GeV. The meanings of symbols and curves are the same as those in Fig. 1. In the calculation, the parameter values obtained by fitting the experimental data are $T = 170$ MeV, $\Delta y = \delta y = 0.595$, and $Dy = 1.340$. For the centrality cuts from 0–5% to 39–81%, the contributions of leading projectile or target protons are taken as $k = 0.06$, 0.08, 0.12, 0.19, and 0.28 with χ^2/dof of 0.158, 0.118, 0.174, 0.130, and 0.386, respectively.

From the above figures one can see that the values of parameters T, Δy, δy, and Dy increase with increasing the incident energy; and do not depend on the centrality cut for a given incident energy. The contribution of leading protons increases with decreasing the centrality. Different distribution shapes of proton rapidity are effected by the different contributions of leading protons. From $\Delta y = \delta y$ we know that there is no overlap or gap between

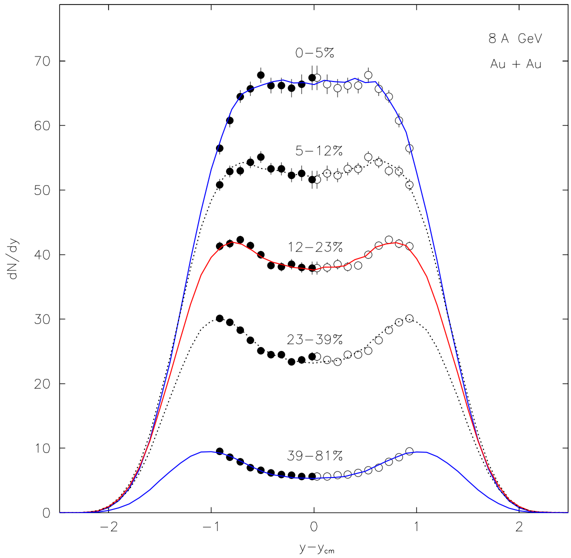

Fig. 2. Rapidity distribution of protons produced in Au–Au collisions at 8AGeV. The full circles are the experimental data measured by the E917 Collaboration [29] and the open circles are reflected around $y = y_{\rm cm}$ [29]. The curves are our calculated results.

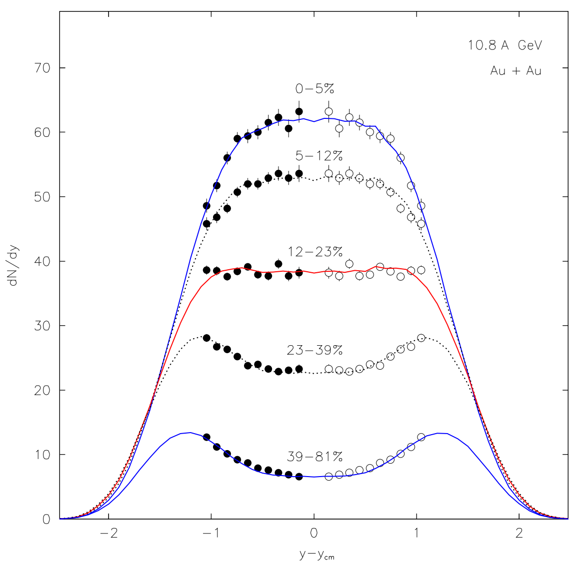

Fig. 3. Rapidity distribution of protons produced in Au–Au collisions at 10.8AGeV. The full circles are the experimental data measured by the E917 Collaboration [29] and the open circles are reflected around $y = y_{\rm cm}$ [29]. The curves are our calculated results.

the projectile and target cylinders. The two cylinders become a long one. If $\Delta y > \delta y$, there is a gap between the two cylinders. If $\Delta y < \delta y$, there is an overlap between the two cylinders.

In order to see the difference between contributions of cylinders and leading protons. Figure 4 shows separately the contributions of cylinders and leading protons. The experimental data (circles) and the parameter values are the same as those in Fig. 3. For the centrality cuts from 0–5% to 39–81%, the contributions of cylinders are given in the figure around central rapidity range by the solid, dotted, dashed, and dotted–dashed curves, as well as small points, respectively. Correspondingly, the contributions of leading protons are given in the figure around fragmentation regions by the same style curves and points. One can see that there are two mixed regions between the two kinds of contributions.

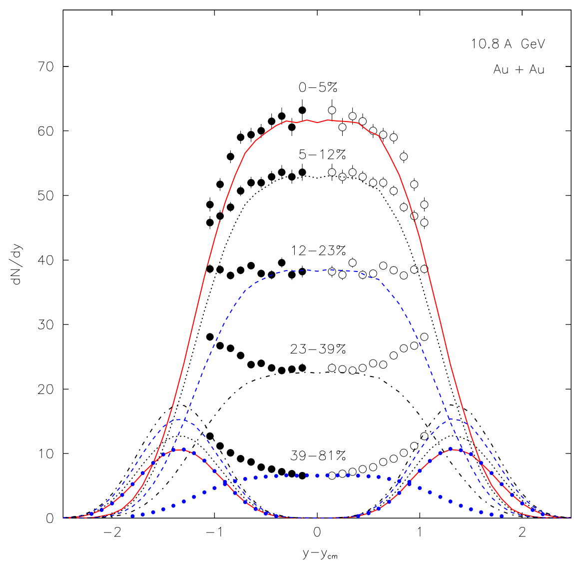

Fig. 4. Comparison between contributions of cylinders and leading protons. The circles are the experimental data of the E917 Collaboration [29] as those shown in Fig. 3. The curves and small points are our calculated results with the same parameter values as those used in Fig. 3.

In order to see the sensitivity of parameters, we change the parameter value by plus or minus 10% and give a recalculation. Figure 5 shows the results of our recalculation for 10.8AGeV Au–Au collisions. The experimental data (circles) are the same as those in Fig. 3. For the five centrality cuts, the results of $0.9T(1.1T)$, $0.9\Delta y(1.1\Delta y)$, $0.9\delta y(1.1\delta y)$, $0.9Dy(1.1Dy)$, and $0.9k(1.1k)$ are given in the figure by the solid, dotted, thin-dashed, thick-dashed, and dotted–dashed curves, respectively, where the values of T, Δy,

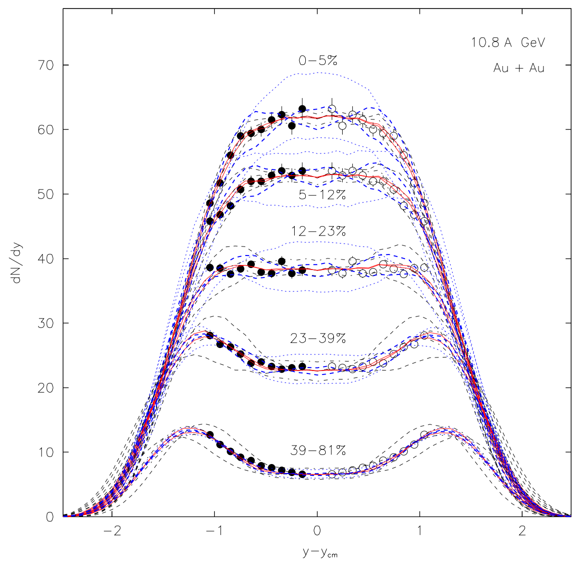

Fig. 5. Sensitivity of the parameter values used in Fig. 3. The circles are the experimental data of the E917 Collaboration [29] as those shown in Fig. 3. The curves are our calculated results.

δy, Dy, and k are the same as those for Fig. 3. From the figure one can see that the calculated results are insensitive to T for the five centrality cuts, to Δy for the last centrality cut, to δy for the last two centrality cuts, to Dy for the first centrality cut, and to k for the five centrality cuts. In short, the rapidity distribution shapes in central and semi-central collisions are sensitive to the rapidity shifts Δy and δy, while the rapidity distribution shapes in non-central collisions are sensitive to the rapidity shift Dy.

The values of Δy and δy define the position relation between the projectile and target cylinders. If $\Delta y = \delta y$, there is no gap or overlap between the two cylinders, the two cylinders become a long one and the present model becomes the previous cylinder model [22–24]. If $\Delta y > \delta y$, there is a gap between the two cylinders, the present model becomes the previous two-cylinder model [25–27]. If $\Delta y < \delta y$, there is an overlap between the two cylinders, the present model becomes the previous overlapping cylinder model [28].

To conclude, we have investigated the dependence of proton rapidity distribution on centrality in Au–Au collisions at 6, 8, and 10.8AGeV by using the two-cylinder model. The model gives a good description of the experimental data measured by the E917 Collaboration. The cylinder length does not depend on the centrality, while the contribution of leading protons increases with the decrease of centrality. The rapidity distribution shape in central and semi-central collisions are sensitive to the rapidity shift Δy and δy, while the rapidity distributions in non-central collisions are sensitive to the leading proton rapidity shift Dy.

This work was supported by the National Natural Science Foundation of China (NSFC) Grant No. 10275042, the Shanxi Provincial Foundation for Returned Overseas Scholars Grant No. JLGB(2001)15, the Shanxi Provincial Foundation for Natural Sciences Grant No. 20021006, and the Shanxi Provincial Foundation for Key Subjects Grant No. JJJC(2002)4.

REFERENCES

[1] M.C. Abreu *et al.*, *Phys. Lett.* **B530**, 33 (2002).

[2] G. Singh, K. Sengupta, P.L. Jain, *Phys. Rev. Lett.* **61**, 1073 (1988).

[3] M.I. Adamovich *et al.* (EMU01 Collaboration), *Phys. Rev. Lett.* **62**, 2801 (1989).

[4] R. Albrecht *et al.*, *Z. Phys.* **C55**, 539 (1992).

[5] P.L. Jain, G. Singh, K. Sengupta, *Phys. Rev.* **C43**, 2027 (1999).

[6] I. Arsene *et al.*, *Phys. Rev. Lett.* **91**, 072305 (2003).

[7] L. Ahle *et al.* (E802 Collaboration), *Phys. Rev.* **C59**, 2173 (1999).

[8] L. Ahle *et al.* (E802 Collaboration), *Phys. Rev.* **C60**, 064901 (1999).

[9] B.B. Back *et al.* (E917 Collaboration), *Phys. Rev. Lett.* **86**, 1970 (2001).

[10] J.I. Nystrand *et al.*, *Nucl. Phys.* **A566**, 419c (1994).

[11] M.I. Adamovich *et al.* (EMU01 Collaboration), *Phys. Lett.* **B201**, 397 (1988).

[12] M.I. Adamovich *et al.* (EMU01 Collaboration), *Phys. Lett.* **B227**, 285 (1989).

[13] R.J. Glauber, in *Lectures of Theoretical Physics*, Vol. 1 eds W.E. Brittin, L.G. Dunham, Interscience, New York 1959, p. 315.

[14] M. Gyulassy, X. N. Wang, *Comput. Phys. Commun.* **83**, 307 (1994).

[15] X.N. Wang, M. Gyulassy, *Phys. Rev. Lett.* **68**, 1480 (1992).

[16] Z.W. Lin, C.M. Ko, *Phys. Rev.* **C68**, 054904 (2003).

[17] Z.W. Lin, S. Pal, C.M. Ko, B.A. Li, B. Zhang, *Nucl. Phys.* **A698**, 375 (2002).

[18] A. Jahns *et al.*, *Z. Phys.* **A341**, 243 (1992).

[19] H. Sorge, *Phys. Rev.* **C52**, 3291 (1995).

[20] G.D. Westfall *et al.*, *Phys. Rev. Lett.* **37**, 1202 (1976).

[21] A. D'innocenzo, G. Ingrosso, P. Rotelli, *Nuovo Cim.* **A55**, 417 (1980).

[22] F.H. Liu, Y.A. Panebratsev, *Nucl. Phys.* **A641**, 379 (1998).

[23] F.H. Liu, Y.A. Panebratsev, *Phys. Rev.* **C59**, 1193 (1999).

[24] F.H. Liu, Y.A. Panebratsev, *Phys. Rev.* **C59**, 1798 (1999).

[25] F.H. Liu, *Phys. Rev.* **C66**, 047902 (2002).

[26] F.H. Liu, D.H. Zhang, M.Y. Duan, *Europhys. Lett.* **61**, 736 (2003).

[27] F.H. Liu, X.Y. Yin, J.L. Tian, N.N. Abd Allah, *Phys. Rev.* **C69**, 034905 (2004).

[28] F.H. Liu, *Phys. Lett.* **B583**, 68 (2004).

[29] B.B. Back *et al.* (E917 Collaboration), *Phys. Rev.* **C66**, 054901 (2002).

[30] C.Y. Wong, *Introduction to High-Energy Heavy-Ion Collisions*, World Scientific, Singapore 1994, p. 25; *Gaoneng Zhonglizi Pengzhuang Daolun*, chinese edition, Harbin Institute of Technology Press, Harbin, China 2002, p. 23.